

BRCA1/BARD1 Orthologs Required for DNA Repair in *Caenorhabditis elegans*

Simon J. Boulton,^{1,2} Julie S. Martin,¹
Jolanta Polanowska,¹ David E. Hill,²
Anton Gartner,³ and Marc Vidal²

¹DNA Damage Response Laboratory
Cancer Research UK
The London Research Institute
Clare Hall Laboratories
South Mimms EN6 3LD
United Kingdom

²Dana Farber Cancer Institute and
Department of Genetics
Harvard Medical School
1 Jimmy Fund Way
Boston Massachusetts 02115

³Max-Planck-Institute for Biochemistry
D 82152 Martinsried
Am Klopferspitz 18a
Germany

Summary

Inherited germline mutations in the tumor suppressor gene *BRCA1* predispose individuals to early onset breast and ovarian cancer [1]. *BRCA1* together with its structurally related partner *BARD1* is required for homologous recombination and DNA double-strand break repair, but how they perform these functions remains elusive [2, 3]. As part of a comprehensive search for DNA repair genes in *C. elegans*, we identified a *BARD1* ortholog. In protein interaction screens, *Ce-BRD-1* was found to interact with components of the sumoylation pathway, the TACC domain protein *TAC-1*, and most importantly, a homolog of mammalian *BRCA1*. We show that animals depleted for either *Ce-brc-1* or *Ce-brd-1* display similar abnormalities, including a high incidence of males, elevated levels of p53-dependent germ cell death before and after irradiation, and impaired progeny survival and chromosome fragmentation after irradiation. Furthermore, depletion of *ubc-9* and *tac-1* leads to radiation sensitivity and a high incidence of males, respectively, potentially linking these genes to the *C. elegans* *BRCA1* pathway. Our findings support a shared role for *Ce-BRC-1* and *Ce-BRD-1* in *C. elegans* DNA repair processes, and this role will permit studies of the *BRCA1* pathway in an organism amenable to rapid genetic and biochemical analysis.

Results

A host of reports have implicated *BRCA1* in DNA repair processes, a function that may partly explain its role as a tumor suppressor [1, 4, 5]. *BRCA1* was found to interact with *Rad51* and form foci at sites of DNA double

strand breaks (DSBs) generated after genotoxic stress [6]. Subsequently, *BRCA1* was shown to associate with other DNA repair genes, including *BRCA2*, *FANCD2*, and the *Mre11/Rad50/Nbs1* complex [7–9]. Consistent with these findings, cells lacking functional *BRCA1* are defective for DNA DSB repair by homologous recombination [3]. *BRCA1* exists primarily in a heterodimeric form with a structurally related protein *BARD1* (*BRCA1*-associated RING domain 1) [10–12]. Recent studies have shown that the *BRCA1/BARD1* heterodimer possesses ubiquitin E3 ligase activity that is abolished by tumor-derived mutations within the RING domain of *BRCA1* [13–15]. Despite these observations, the precise mechanism through which *BRCA1* functions in DNA repair and tumor suppression remains unknown. Genetic dissection of the *BRCA1* pathway is likely to provide important mechanistic insights into its role in DNA repair processes but has been limited by the apparent absence of *BRCA1* or its partners in yeast, worms, or flies.

As part of a detailed search of the *C. elegans* genome sequence for putative DNA repair genes, we identified a putative ortholog of *BARD1* (K04C2.4, *Ce-brd-1*; Figure 1A). K04C2.4 encodes a protein (*Ce-BRD-1*) of 670 amino acids with 23% identity and 41% similarity to human *BARD1*. Containing a putative N-terminal RING finger domain, three ankyrin repeats in the central region of the protein, and two C-terminal BRCT repeat domains, *Ce-BRD-1* is most related to *Xenopus laevis* *BARD1* (Figure 1A) [16]. Given that *BRCA1* occurs as a heterodimer with *BARD1*, the identification of *Ce-BRD-1* raised the possibility that a *BRCA1* homolog may also exist in the nematode. However, extensive sequence searches of the *C. elegans* genome failed to uncover a potential *BRCA1* homolog.

To identify a *Ce-BRD-1* partner that may perform a function analogous to that of *BRCA1*, we screened for *Ce-BRD-1*-associated proteins by using the yeast two-hybrid system [17]. Among the *Ce-BRD-1*-interacting proteins identified were the ubiquitin-like SMT-3/sumo protein, the E2 sumo-conjugating enzyme *UBC-9*, and a protein of unknown function (*TAC-1*; Y54E2A.3) that contains a TACC domain also present in *AZU1*, a putative breast cancer tumor suppressor (see the Supplemental Data available with this article online) [18]. Most importantly, we identified *Ce-BRC-1* (C36A4.8), a protein of 596 amino acids that is 24% identical and 52% similar to the major human *BRCA1* delta-exon 11 splice variant. Similar to *BRCA1*, *Ce-BRC-1* contains an N-terminal RING finger, a nuclear localization signal, and two C-terminal BRCT repeat domains (Figure 1B). *Ce-BRC-1* was missed in bioinformatic searches of the *C. elegans* genome because of an error by the Genefinder program, which failed to predict three of its exons (Figure 1B).

To confirm the *Ce-BRD-1* interactions with *Ce-BRC-1*, *UBC-9*, and *SMT-3*, we used yeast two-hybrid matrix and in vitro pull-down assays. Our results suggest that *Ce-BRC-1* and *Ce-BRD-1*, similar to their mammalian counterparts [11, 12], interact with each other through their RING domains located at their respective N-termini;

*Correspondence: simon.boulton@cancer.org.uk

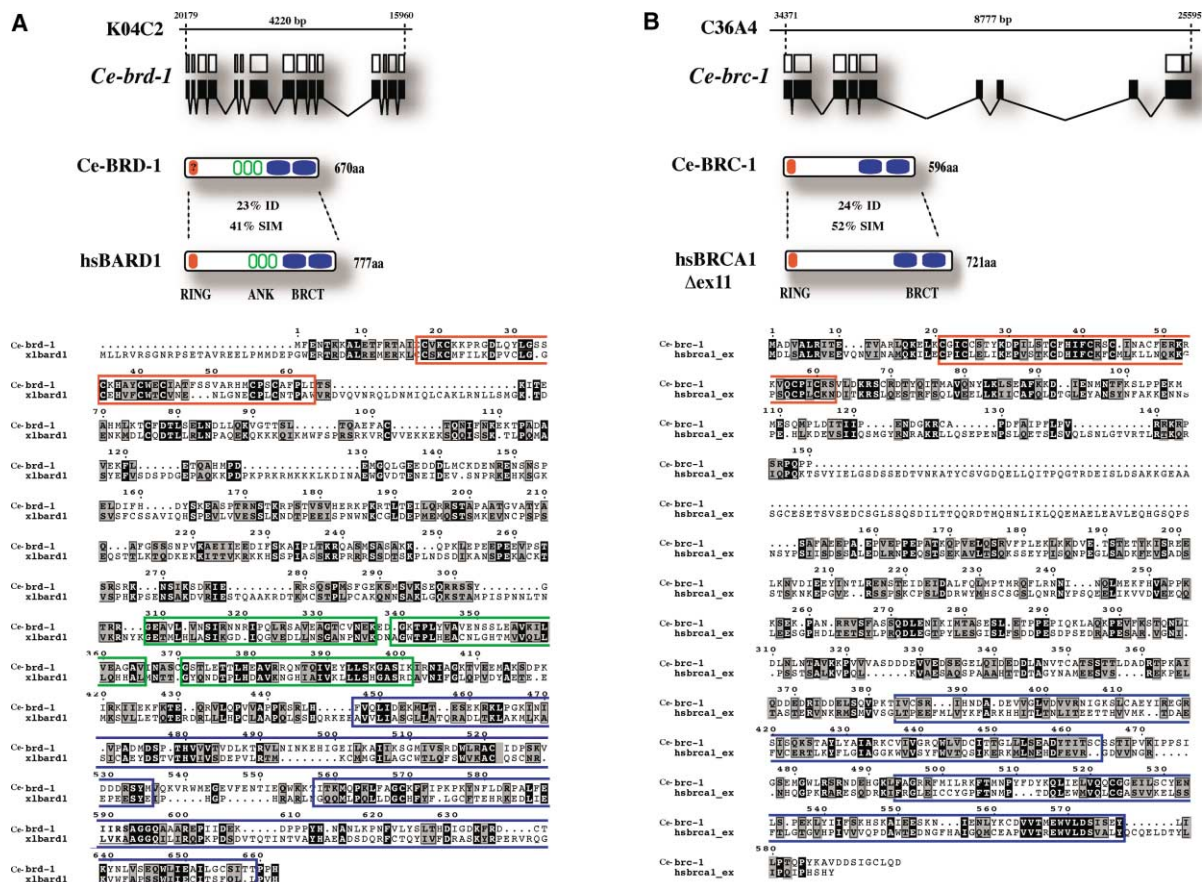


Figure 1. Gene and Domain Structure of Ce-BRC-1 and Ce-BRD-1 and Their Relationship to BRCA1 and BARD1

(A) The gene structure of *Ce-brd-1* (K04C2.4). The upper panel shows a comparison of the predicted intron-exon gene structure (white boxes, exons) of the *Ce-brd-1*-coding locus compared with the confirmed gene structure (black boxes, exons) derived from ORFeome sequencing. *Ce-BRD-1* encodes a 670 amino acid protein with a putative RING finger (red), three ankyrin repeats (green), and two BRCT domains (blue) and is highly related to hsBARD1. Shown in the lower panel is the protein sequence alignment between *Ce-BRD-1* and *X. laevis* BARD1 (xIBARD). The key for colors is as for the domain structure.

(B) The corrected gene structure of *Ce-brc-1* (C36A4.8). Note the three additional, confirmed exons (black) not found in the predicted gene structure (white). *Ce-BRC-1* encodes a 596 amino acid protein with a RING finger (red) and two BRCT domains (blue). Shown in the lower panel is the protein sequence alignment between *Ce-BRC-1* and hsBRCA1 delta exon 11 (hsbrca1_ex). The key for colors is as for the domain structure.

the N-terminal 130 amino acids of *Ce-BRC-1* and *Ce-BRD-1* are sufficient for heterodimerization but do not interact with themselves (Figure 2A). Furthermore, full-length *Ce-BRC-1* and the N-terminal region of *Ce-BRC-1* fused to glutathione S-transferase (GST) can efficiently pull-down the corresponding N-terminal region of *Ce-BRD-1* expressed in vitro (Figure 2B, lanes 2 and 3). Our results imply that this interaction is conserved and suggest that *Ce-BRC-1* and *Ce-BRD-1* may function together as a heterodimer in *C. elegans* but are unlikely to function separately as homodimers. We also found that UBC-9 could efficiently interact with the DNA strand-exchange protein RAD-51 and *Ce-BRD-1* in both the yeast two-hybrid system and in pull-down experiments from tissue culture cells (Figures 2C and 2D, lanes 1 and 4, respectively). Experiments in human cells have shown that BRCA1 can associate with RAD51 in GST pull downs [19]. Our results suggest that the *Ce-BRC-1*/*Ce-BRD-1* heterodimer may associate indirectly with RAD-51 and other proteins involved in homologous re-

combination through their ability to interact with UBC-9 (Figure 2D and Supplemental Data).

To investigate if *Ce-BRC-1* and *Ce-BRD-1* participate in *C. elegans* damage response pathways, we depleted them by using RNA-mediated interference (RNAi) via the RNAi feeding procedure [20, 21]. Under normal growth conditions, depletion of *Ce-brc-1* or *Ce-brd-1* gave rise to elevated levels of chromosome nondisjunction that manifest as a high proportion of males (Him phenotype; the result of X chromosome nondisjunction) in the self progeny. Consistent with a weak Him phenotype, we observed 2.54% (17/670) and 2.88% (23/798) males for *Ce-brc-1*- and *Ce-brd-1*-depleted animals, respectively, in contrast to 0.13% (1/756) males for the RNAi control. *Ce-brc-1*- and *Ce-brd-1*-depleted animals also displayed elevated levels of germ cell death under normal growth conditions (Figure 3A, panels 2, 3, 8, and 9). Using CED-1::GFP as a marker of germ cell death showed the number of corpses in *Ce-brc-1* and *Ce-brd-1* RNAi animals to be 8.2 ± 3.1 ($n = 50$) and $9.4 \pm$

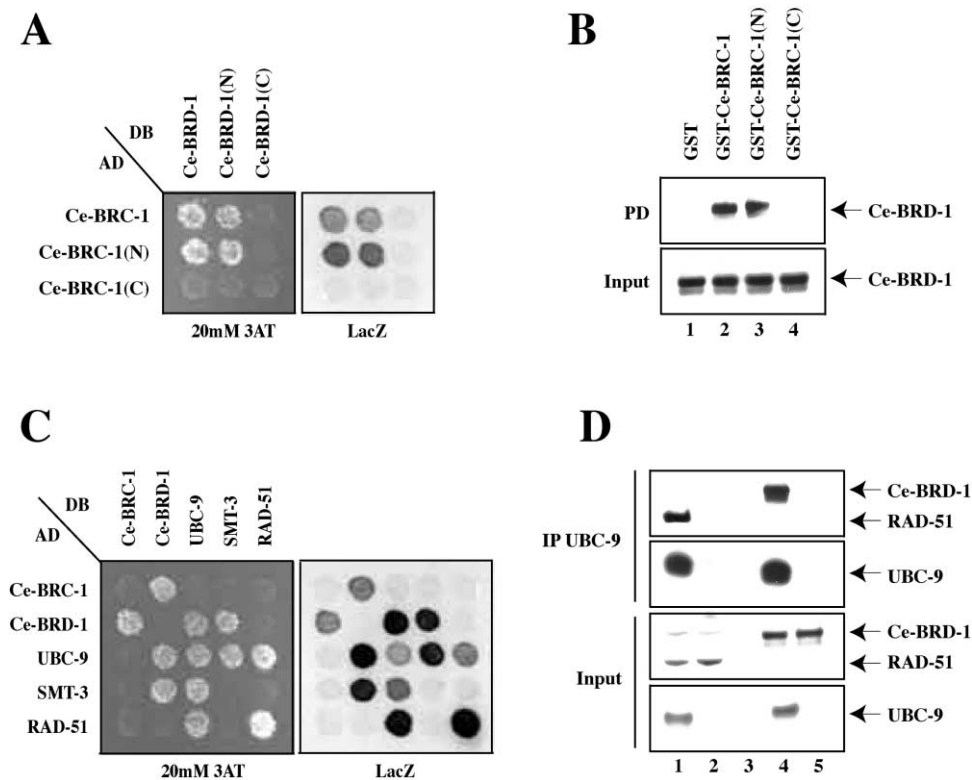


Figure 2. Ce-BRD-1-Interacting Proteins

(A) Ce-BRD-1 and Ce-BRC-1 interact through their respective N-terminal domains. We used the yeast two-hybrid system to test for protein interactions between full-length, N-terminal (amino acids 1–130), and C-terminal (Ce-BRC-1: amino acids 130–602; Ce-BRD-1: amino acids 130–653) fused to either the DNA binding domain (DB) or the activation domain (AD) of GAL4 by scoring for *lacZ* expression and growth on 20 mM 3AT plates.

(B) GST fusions to full-length (lane 2), N-terminal (lane 3), and C-terminal (lane 4) fragments of Ce-BRC-1 were used to pull down an N-terminal Ce-BRD-1 fragment expressed in vitro.

(C) The yeast two-hybrid system was used to test for protein interactions among Ce-BRC-1, Ce-BRD-1, UBC-9, SMT-3, and RAD-51 fused to either the DNA binding domain (DB) or the activation domain (AD) of GAL4.

(D) Myc-tagged UBC-9 was used to pull down 6xHis-tagged Ce-BRD-1 and 6xHis-tagged RAD-51 expressed in 293T cells.

3.8 ($n = 50$) per germline, respectively. In contrast, an average of 1.2 ± 0.5 ($n = 50$) corpses were observed in the wild-type germline under normal growth conditions.

Exposure of *Ce-brc-1*- and *Ce-brd-1*-depleted animals to γ -irradiation at the late L4 stage resulted in dramatically enhanced levels of germ cell death that became evident at the 4 hour time point after irradiation (Figure 3A: panels 5, 6, 11, and 12; Figure 3B) and reached a maximum at the 24 hour time point (Figure 3A: panels 14 and 15; Figure 3B and data not shown). At the latter time point, oocytes were absent, and the general morphology of the germline was severely compromised because of extensive germ cell death (Figure 3A, panels 14 and 15). The hatching rates of progeny from both *Ce-brc-1*- and *Ce-brd-1*-depleted animals were found to be dramatically reduced after exposure to γ -irradiation when these animals were compared to RNAi controls (Figure 3C), demonstrating that *Ce-brc-1*- and *Ce-brd-1*-depleted animals are radiation sensitive.

To test if the apoptotic phenotype of *Ce-brc-1*- and *Ce-brd-1*-depleted animals observed before and after DNA damage is dependent on an intact DNA damage checkpoint, we used RNAi to measure germ cell corpses

in *cep-1* (*C. elegans* p53) and *rad-5* checkpoint mutants depleted of *Ce-brc-1* and *Ce-brd-1* [22–24]. Both *cep-1* and *rad-5* mutations were found to suppress the elevated number of apoptotic corpses in *Ce-brc-1* or *Ce-brd-1* RNAi animals before and after irradiation (Figure 4A). These results demonstrate that the enhanced apoptotic phenotype observed in *Ce-brc-1*- and *Ce-brd-1*-depleted animals, both before and after exposure to γ -irradiation, requires an intact DNA damage checkpoint.

To analyze chromosome integrity after irradiation of *Ce-brc-1*- or *Ce-brd-1*-depleted animals, we used DAPI staining to visualize germline nuclei after treatment of late L4 stage animals with γ -irradiation. In contrast to controls, germlines isolated from irradiated *Ce-brc-1*- or *Ce-brd-1*-depleted animals displayed evidence of abnormal chromosome morphology and fragmentation in transition zone and pachytene nuclei (Figure 4B). Chromosomes appeared brittle and frayed, and in many nuclei small DNA fragments could be seen broken off from the main body of chromatin (Figure 4B, panels 3–6).

Similar to RNAi of *Ce-brc-1*- and *Ce-brd-1*-depleted worms, RNAi of *tac-1* (Y54E2A.3) also gave rise to a Him

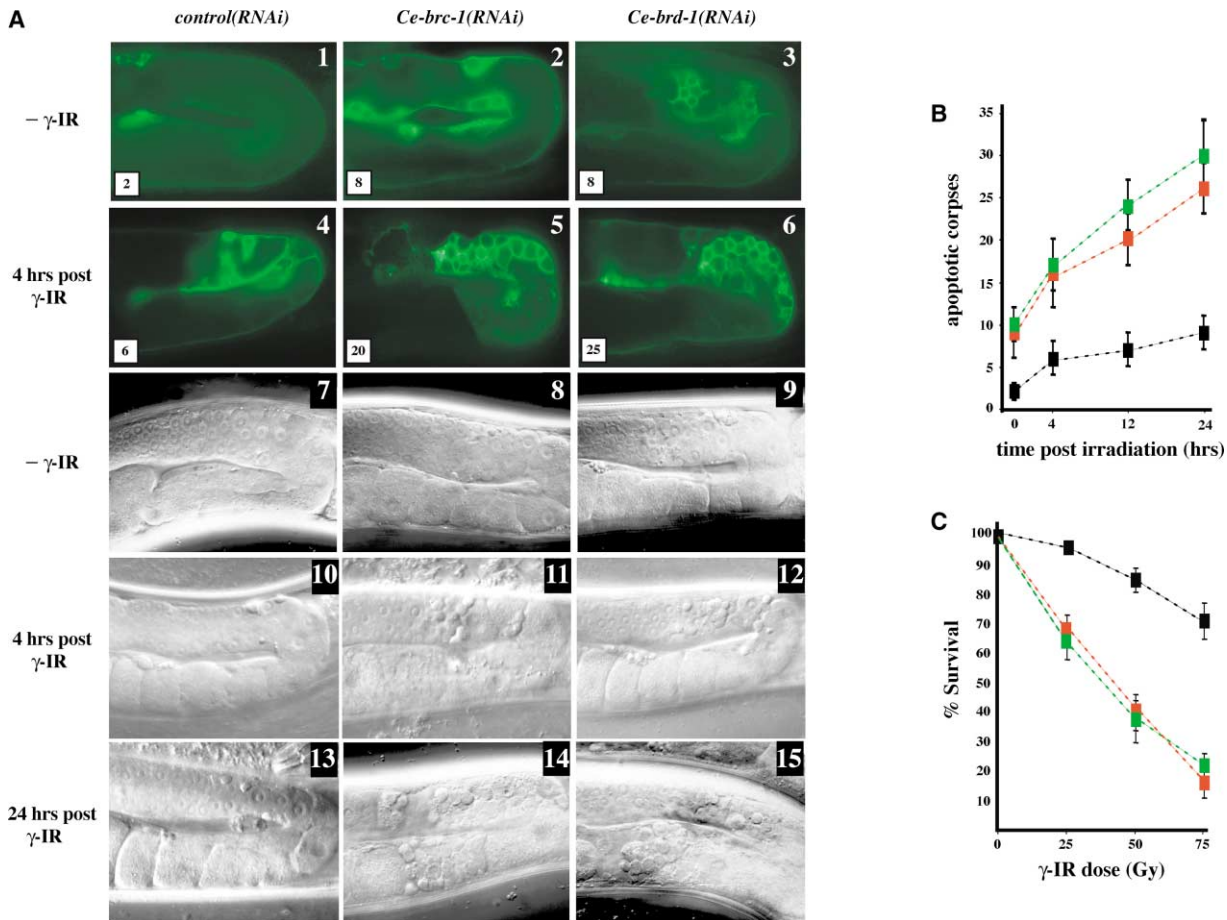


Figure 3. Phenotypes of *Ce-brc-1*- and *Ce-brd-1*-Depleted Animals after Treatment with DNA-Damaging Agents

(A) Enhanced radiation induced death after depletion of *Ce-brc-1* or *Ce-brd-1*. Shown is a representative image of the meiotic pachytene region of RNAi-treated animals (\pm 75 Gy γ -irradiation) at the indicated time points after irradiation. Apoptotic corpses in the pachytene region of the germline were visualized in CED-1::GFP transgenic animals as a ring of GFP fluorescence surrounding dying cells (panels 1–6) or as refractile bodies seen under Nomaski optics (panels 7–15). The number of apoptotic corpses is indicated in the bottom left corner of panels 1–6. Panel numbers are indicated in the top right corner of each image.

(B) Apoptotic corpses were counted at 4, 12, and 24 hours after irradiation (75 Gy) in 20 animals for each data point. Error bars indicate SEM (standard error of the mean).

(C) Shown is the percent survival of progeny after exposure to the indicated doses of γ -irradiation. Error bars indicate SEM. Wild-type = black; *Ce-brc-1(RNAi)* = green; *Ce-brd-1(RNAi)* = red.

phenotype (4.26% males [38/892]; see Supplemental Data), raising the possibility that Ce-BRC-1, Ce-BRD-1, and TAC-1 may function in a common pathway. Consistent with a requirement for sumoylation in many biological processes, RNAi of the sumo-conjugating enzyme *ubc-9* resulted in a pleiotropic phenotype that included sterility and embryonic lethality under normal growth conditions. After γ -irradiation, *ubc-9*-depleted animals also displayed enhanced germ cell death, demonstrating that *ubc-9(RNAi)* animals have radiation sensitivity similar to that of *Ce-brc-1*- and *Ce-brd-1*-depleted animals (see Supplemental Data).

Discussion

The results presented here reveal the unanticipated discovery of functional orthologs of the BRCA1 tumor suppressor gene and its partner BARD1 in *C. elegans*. The

importance of these findings is underscored by the absence of BRCA1/BARD1 homologs in fungus and fruit fly genomes. *Ce-brd-1* encodes a protein with amino acid identity and size similar to that of BARD1. However, *Ce-brc-1* encodes a more divergent protein that is significantly shorter than BRCA1 but is most related to its exon delta 11 splice variant. The fact that sequences resembling BRCA1 exon 11 are absent from the *C. elegans* genome raises the possibility that some functions of human BRCA1 may not be performed by either Ce-BRC-1 or related factors in trans.

Our analyses suggest that *Ce-brc-1* and *Ce-brd-1* function together in a common DNA repair pathway, consistent with the role of BRCA1 and BARD1 in mammalian cells. First, we demonstrate that Ce-BRC-1 and Ce-BRD-1 physically interact in vitro via conserved domains that are also responsible for mediating the human BRCA1-BARD1 interaction [12, 25]. Second, *Ce-brc-1*-

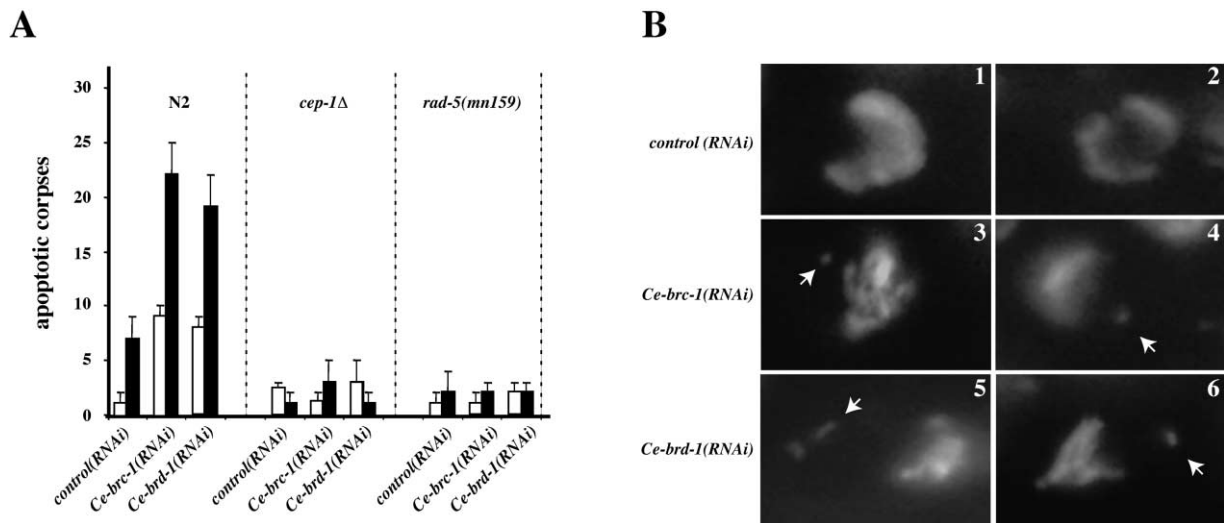


Figure 4. Checkpoint-Dependent Apoptosis and Chromosomal Fragmentation in *Ce-brc-1*- and *Ce-brd-1*-Depleted Animals

(A) Enhanced germ cell death in the absence of *Ce-brc-1* or *Ce-brd-1* before and after irradiation is checkpoint dependent. Apoptotic corpses before (white bars) and after (black bars) γ -irradiation were counted in wild-type N2, *cep-1(gk138)* and *rad-5(mn159)* mutants after RNAi depletion with control, *Ce-brc-1*, and *Ce-brd-1* RNAi constructs. In both cases, *cep-1(gk138)* and *rad-5(mn159)* suppressed the number of apoptotic corpses after *Ce-brc-1* and *Ce-brd-1* RNAi to near wild-type levels. Twenty germlines were scored for each data point.

(B) IR-induced chromosomal defects in the absence of *Ce-brc-1* or *Ce-brd-1*. L4 larval stage control, *Ce-brc-1*, and *Ce-brd-1* RNAi animals were treated with 20 Gy of γ -irradiation. Shown are two representative images of DAPI-stained germline nuclei in control (panels 1 and 2), *Ce-brc-1* (panels 3 and 4), or *Ce-brd-1* (panels 5 and 6) RNAi animals 16 hrs after treatment. Chromosomes in *Ce-brc-1*- or *Ce-brd-1*-depleted animals (panels 3–6) have an abnormal frayed appearance, and DNA fragments that are physically distinct from the main body of DAPI-stained chromatin are apparent (arrows). Chromosomal abnormalities or DNA fragments were observed in individual nuclei at the following frequencies: control RNAi (3/228); *Ce-brc-1* (32/204); and *Ce-brd-1* (47/263).

and *Ce-brd-1*-depleted animals display very similar phenotypes that are highly reminiscent of the phenotype of human cells lacking *BRCA1* [2]. We find that *Ce-brc-1*- and *Ce-brd-1*-depleted animals gave rise to a Him phenotype (increased levels of X-chromosome non-disjunction) that could be caused by a defect during meiotic prophase or by a premeiotic chromosome segregation defect. Cytological analysis of *Ce-brc-1*- and *Ce-brd-1*-depleted animals failed to unambiguously identify the defect(s) responsible for this phenotype, suggesting that a detailed study of loss-of-function mutants in *Ce-brc-1* and *Ce-brd-1* genes will be required to reconcile this phenotype. Under normal growth conditions, we also observed increased checkpoint-dependent germ cell death after depletion of *Ce-brc-1* or *Ce-brd-1*. This suggests that unrepaired DNA damage or aberrant chromosome structures that lead to checkpoint activation accumulate after *Ce-brc-1* or *Ce-brd-1* depletion. Finally, we show that treatment of *Ce-brc-1*- or *Ce-brd-1*-depleted animals with γ -irradiation results in increased germ cell death, radiation sensitivity, and chromosome fragmentation. Together, these phenotypes strongly suggest that *Ce-BRC-1* and *Ce-BRD-1* are required for DNA repair in *C. elegans*.

SMT-3, UBC-9, and TAC-1 were also identified as *Ce-BRD-1*-interacting proteins. We have shown that *ubc-9* and *tac-1* RNAi depletion results in radiation sensitivity and a Him phenotype, respectively (see Supplemental Data). Although further analysis will be required to conclusively demonstrate both a physical and a genetic link among *Ce-BRC-1*/*Ce-BRD-1*, TAC-1, and components of the sumoylation pathway, it is tempting to speculate

that these genes function together or regulate a common pathway. Indeed, a *Ce-BRC-1*/*Ce-BRD-1*/*UBC-9* complex could function in DNA repair processes by ubiquitylating/sumoylating common targets required for DNA repair processes. Such posttranslational modifications could be important for modulating the activities of repair proteins at the sites of DNA damage, as has been described recently for budding yeast PCNA [26].

In summary, the existence of *BRCA1* and *BARD1* orthologs in *C. elegans*, an organism amenable to high-throughput genetic manipulation via genome-wide RNAi libraries [38, 39], together with the observation that other *BRCA1* pathway components, including orthologs of *FANCD2* and *BACH1* ([27]; S.B., J.M., and J.P., unpublished data), are conserved in *C. elegans*, suggests that genetic and biochemical dissection of the *BRCA1*/*BARD1* pathway in the nematode will lead to important insights into its role in human disease.

Experimental Procedures

Worm Strains

C. elegans strains were cultured as described previously [29]. The following strains were kindly provided by the *Caenorhabditis* Genetics Center (University of Minnesota, St. Paul, MN): wild-type Bristol N2, *cep-1(gk138)*, a deletion in the *C. elegans* homolog of p53, and SP506 *rad-5(mn159)*. MD701 *bcls39 V [Plim-7::CED-1::GFP]* was kindly provided by Barbara Conratt.

Sequence Alignments

Protein sequences were aligned by pileup and refined via the lineup algorithm (Genetics Computer Group). Multiple sequence files were exported to ESPrpt 2.0 at http://prodes.toulouse.inra.fr/ESPrpt/cgi-bin/nph-ESPrpt_exe.cgi for box-shading analysis.

Gateway Recombinational Cloning

ORF-specific primers compatible with the Gateway system [30, 31] were designed to full-length Genefinder ORF predictions and cloned into Entry as previously described. Primer sequences for cloning K04C2.4 (*Ce-brd-1*) can be found at <http://worfdb.dfci.harvard.edu/search.pl?form=1&search=K04C2.4>, and those for C36A4.8 (*Ce-brc-1*) can be found at <http://worfdb.dfci.harvard.edu/search.pl?form=1&search=C36A4.8> [32]. ORFs were transferred by LR destination cloning, as previously described [28], into pAD-Amp, pDB-Gent (for yeast-two hybrid analysis), pEXP1 (for in vitro transcription/translation), pGST (for GST-fusion pull-down assays), L4440-dest (for RNAi by feeding), pDEST-CMV-Myc, and pDEST-CMV_6xHis (protein expression in 293T cells).

Yeast Two-Hybrid and Interaction Assays

The yeast two-hybrid methods used were as previously described. To test pairwise interactions in yeast, we used Gal4 DNA binding domain (DB) and activation domain (AD) fusions to cotransform MAV103 yeast. We tested interactions for each combination by scoring for yeast two-hybrid phenotypes (LacZ, -Ura) at 30°C as described previously [33]. For GST pull-down experiments, ³⁵S-M labeled BRD-1N in vitro translations (Ambion) were incubated with 500 ng of GST-fusion protein (GST, GST-Ce-BRC-1, GST-Ce-BRC-1(N), and GST-Ce-BRC-1(C)) on Sepharose beads for 30 min at 4°C before being washed three times with ELB250 (50 mM HEPES [pH 7.0], 250 mM NaCl, 0.5% NP-40, 0.5 mM EDTA, 1 mM PMSF, 0.5 mM NaF, 0.1 mM Na₂VO₃, 0.5 mM DTT, and protease inhibitor cocktail [Invitrogen]). Proteins associated with the beads were subjected to electrophoresis and radiography. 293T cells were transiently transfected with pDEST-CMV-Myc-UBC-9, pDEST-CMV_6xHis-Ce-BRD-1, and pDEST-CMV_6xHis-RAD-51 constructs via LipofectAMINE 2000 (Gibco BRL). Seventy-two hours after transfection, cells were harvested and lysed in ELB250 (50 mM HEPES [pH 7.0], 250 mM NaCl, 0.5% NP-40, 0.5 mM EDTA, 1 mM PMSF, 0.5 mM NaF, 0.1 mM Na₂VO₃, 0.5 mM DTT, and protease inhibitor cocktail [Invitrogen]) prior to clarification of extracts via a 42K spin in a Beckman ultracentrifuge for 30 min. Extracts were incubated with 9E10 antibodies coupled to beads for 30 min at 4°C before being washed three times with ELB250. Proteins associated with the beads were subjected to electrophoresis and then Western blotting with 9E10 (a-Myc) and 6xHis antibodies (Amersham).

Gene Knockdown

RNAi depletion by the feeding method was performed as described previously [20, 28]. In brief, HT115(DE3) bacteria containing the appropriate RNAi feeding construct were spread on Luria-Broth (LB) plates containing ampicillin (Amp) and incubated overnight at 37°C. The resulting bacterial lawns were suspended in 200 μl LB, and 50 μl from these suspensions were seeded in the wells of 6-well nematode growth media Amp plates containing 6 mM isopropylthio-β-D-galactosidase (Sigma, UK). For each RNAi experiment, two P0 L4 worms of the appropriate genotype were picked, transferred to wells, and incubated at 15°C for 72 hours. Three L4 F1 progeny were then transferred to new plates containing fresh bacterial lawns and allowed to lay eggs for 24 hours at 20°C. F2 progeny were analyzed for loss-of-function phenotypes as described in the text. Late L4 progeny were irradiated and analyzed at the indicate time points.

Cytological Preparation and Staining

Gonads were extruded from adult hermaphrodites in 10 μl of phosphate-buffered saline on a poly-L-lysine-coated slide. An equal volume of 7.5% formaldehyde was added, and the tissues were gently squashed under a coverslip, prior to being frozen in liquid N₂ for 5 min. After removal of the coverslips, slides were submerged for 5 min each in methanol, methanol:acetone 1:1, and then acetone at -20°C. For DAPI staining, slides were mounted in vectashield antifading medium (Vector laboratories Inc., Burlingame, CA) containing DAPI (2 ug/ul). Cytological studies were performed with either a Zeiss Axioskop II Mot fluorescence microscope driven by Openlab 3 software (Improvision, Viscount Centre II, Coventry, UK) or a Zeiss LSM510 Meta confocal microscope.

Supplemental Data

Supplemental Data are available with this article online at <http://www.current-biology.com/cgi/content/full/14/1/33/DC1/>.

Acknowledgments

We wish to extend thanks to Barbara Conradt for providing MD701 [*P_{lin-7}-ced-1::gfp*] and to the Caenorhabditis Genetic center and Alan Coulson for providing *C. elegans* strains and cosmids, respectively. Thank go to Steve West and Juliet Reid for comments on the manuscript. We are also grateful to members of Cancer Research UK, Clare Hall Laboratories and to the Vidal and Livingston labs for helpful discussions. A.G. was supported by the Max Planck Society (E. Nigg) and by Deutsche Forschungsgemeinschaft grants DFG 701-1/1 and 702-1/1. M.V. was supported by grants 5R01HG01715-02 (National Human Genome Research Institute), P01CA80111-02, 7 R33 CA81658-02 (National Cancer Institute), and 232 (Merck Genome Research Institute). S.B., J.M., and J.P. are funded by Cancer Research UK.

Received: August 21, 2003

Revised: October 14, 2003

Accepted: November 6, 2003

Published: January 6, 2004

References

1. Venkitaraman, A.R. (2002). Cancer susceptibility and the functions of BRCA1 and BRCA2. *Cell* 108, 171–182.
2. Scully, R., Ganesan, S., Vlasakova, K., Chen, J., Socolovsky, M., and Livingston, D.M. (1999). Genetic analysis of BRCA1 function in a defined tumor cell line. *Mol. Cell* 4, 1093–1099.
3. Moynahan, M.E., Chiu, J.W., Koller, B.H., and Jasin, M. (1999). Brca1 controls homology-directed DNA repair. *Mol. Cell* 4, 511–518.
4. Scully, R., and Livingston, D.M. (2000). In search of the tumour-suppressor functions of BRCA1 and BRCA2. *Nature* 408, 429–432.
5. Chen, Y., Lee, W.H., and Chew, H.K. (1999). Emerging roles of BRCA1 in transcriptional regulation and DNA repair. *J. Cell. Physiol.* 181, 385–392.
6. Scully, R., Chen, J., Ochs, R.L., Keegan, K., Hoekstra, M., Feunteun, J., and Livingston, D.M. (1997). Dynamic changes of BRCA1 subnuclear location and phosphorylation state are initiated by DNA damage. *Cell* 90, 425–435.
7. Taniguchi, T., Garcia-Higuera, I., Andreassen, P.R., Gregory, R.C., Grompe, M., and D'Andrea, A.D. (2002). S-phase-specific interaction of the Fanconi anemia protein, FANCD2, with BRCA1 and RAD51. *Blood* 100, 2414–2420.
8. Zhong, Q., Chen, C.F., Li, S., Chen, Y., Wang, C.C., Xiao, J., Chen, P.L., Sharp, Z.D., and Lee, W.H. (1999). Association of BRCA1 with the hRad50-hMre11-p95 complex and the DNA damage response. *Science* 285, 747–750.
9. Chen, J., Silver, D.P., Walpita, D., Cantor, S.B., Gazdar, A.F., Tomlinson, G., Couch, F.J., Weber, B.L., Ashley, T., Livingston, D.M., et al. (1998). Stable interaction between the products of the BRCA1 and BRCA2 tumor suppressor genes in mitotic and meiotic cells. *Mol. Cell* 2, 317–328.
10. Wu, L.C., Wang, Z.W., Tsan, J.T., Spillman, M.A., Phung, A., Xu, X.L., Yang, M.C., Hwang, L.Y., Bowcock, A.M., and Baer, R. (1996). Identification of a RING protein that can interact in vivo with the BRCA1 gene product. *Nat. Genet.* 14, 430–440.
11. Brzovic, P.S., Rajagopal, P., Hoyt, D.W., King, M.C., and Klevit, R.E. (2001). Structure of a BRCA1-BARD1 heterodimeric RING-RING complex. *Nat. Struct. Biol.* 8, 833–837.
12. Meza, J.E., Brzovic, P.S., King, M.C., and Klevit, R.E. (1999). Mapping the functional domains of BRCA1. Interaction of the ring finger domains of BRCA1 and BARD1. *J. Biol. Chem.* 274, 5659–5665.
13. Baer, R., and Ludwig, T. (2002). The BRCA1/BARD1 heterodimer, a tumor suppressor complex with ubiquitin E3 ligase activity. *Curr. Opin. Genet. Dev.* 12, 86–91.
14. Chen, A., Kleiman, F.E., Manley, J.L., Ouchi, T., and Pan, Z.Q.

- (2002). Autoubiquitination of the BRCA1*BARD1 RING ubiquitin ligase. *J. Biol. Chem.* 277, 22085–22092.
15. Mallery, D.L., Vandenberg, C.J., and Hiom, K. (2002). Activation of the E3 ligase function of the BRCA1/BARD1 complex by polyubiquitin chains. *EMBO J.* 21, 6755–6762.
 16. Joukov, V., Chen, J., Fox, E.A., Green, J.B., and Livingston, D.M. (2001). Functional communication between endogenous BRCA1 and its partner, BARD1, during *Xenopus laevis* development. *Proc. Natl. Acad. Sci. USA* 98, 12078–12083.
 17. Du, W., Vidal, M., Xie, J.E., and Dyson, N. (1996). RBF, a novel RB-related gene that regulates E2F activity and interacts with cyclin E in *Drosophila*. *Genes Dev.* 10, 1206–1218.
 18. Chen, H.M., Schmeichel, K.L., Mian, I.S., Lelievre, S., Petersen, O.W., and Bissell, M.J. (2000). AZU-1: a candidate breast tumor suppressor and biomarker for tumor progression. *Mol. Biol. Cell* 11, 1357–1367.
 19. Scully, R., Chen, J., Plug, A., Xiao, Y., Weaver, D., Feunteun, J., Ashley, T., and Livingston, D.M. (1997). Association of BRCA1 with Rad51 in mitotic and meiotic cells. *Cell* 88, 265–275.
 20. Fire, A., Xu, S., Montgomery, M.K., Kostas, S.A., Driver, S.E., and Mello, C.C. (1998). Potent and specific genetic interference by double-stranded RNA in *Caenorhabditis elegans*. *Nature* 391, 806–811.
 21. Timmons, L., and Fire, A. (1998). Specific interference by ingested dsRNA. *Nature* 395, 854.
 22. Ahmed, S., Alpi, A., Hengartner, M.O., and Gartner, A. (2001). *C. elegans* RAD-5/CLK-2 defines a new DNA damage checkpoint protein. *Curr. Biol.* 11, 1934–1944.
 23. Derry, W.B., Putzke, A.P., and Rothman, J.H. (2001). *Caenorhabditis elegans* p53: role in apoptosis, meiosis, and stress resistance. *Science* 294, 591–595.
 24. Schumacher, B., Hofmann, K., Boulton, S., and Gartner, A. (2001). The *C. elegans* homolog of the p53 tumor suppressor is required for DNA damage-induced apoptosis. *Curr. Biol.* 11, 1722–1727.
 25. Morris, J.R., Keep, N.H., and Solomon, E. (2002). Identification of residues required for the interaction of BARD1 with BRCA1. *J. Biol. Chem.* 277, 9382–9386.
 26. Hoeghe, C., Pfander, B., Moldovan, G.L., Pyrowolakis, G., and Jentsch, S. (2002). RAD6-dependent DNA repair is linked to modification of PCNA by ubiquitin and SUMO. *Nature* 419, 135–141.
 27. Timmers, C., Taniguchi, T., Hejna, J., Reifsteck, C., Lucas, L., Bruun, D., Thayer, M., Cox, B., Olson, S., D'Andrea, A.D., et al. (2001). Positional cloning of a novel Fanconi anemia gene, FANCD2. *Mol. Cell* 7, 241–248.
 28. Boulton, S.J., Gartner, A., Reboul, J., Vaglio, P., Dyson, N., Hill, D.E., and Vidal, M. (2002). Combined functional genomic maps of the *C. elegans* DNA damage response. *Science* 295, 127–131.
 29. Brenner, S. (1974). The genetics of *Caenorhabditis elegans*. *Genetics* 77, 71–94.
 30. Walhout, A.J., Temple, G.F., Brasch, M.A., Hartley, J.L., Lorson, M.A., van den Heuvel, S., and Vidal, M. (2000). GATEWAY recombinational cloning: application to the cloning of large numbers of open reading frames or ORFeomes. *Methods Enzymol.* 328, 575–592.
 31. Hartley, J.L., Temple, G.F., and Brasch, M.A. (2000). DNA cloning using *in vitro* site-specific recombination. *Genome Res.* 10, 1788–1795.
 32. Reboul, J., Vaglio, P., Rual, J.F., Lamesch, P., Martinez, M., Armstrong, C.M., Li, S., Jacotot, L., Bertin, N., Janky, R., et al. (2003). *C. elegans* ORFeome version 1.1: experimental verification of the genome annotation and resource for proteome-scale protein expression. *Nat. Genet.* 34, 35–41.
 33. Walhout, A.J., Sordella, R., Lu, X., Hartley, J.L., Temple, G.F., Brasch, M.A., Thierry-Mieg, N., and Vidal, M. (2000). Protein interaction mapping in *C. elegans* using proteins involved in vulval development. *Science* 287, 116–122.